E-ISSN: 3068-5052
Journal of Regenerative Medicine & Biology Research

ATHENAEUM SCIENTIFIC PUBLISHERS

Research Article

CMFlex® Bone Graft Accelerates Bone Formation and Contour Recovery in Multi-Centimeter Porcine Mandibular Defects: A Pilot Study

Derek J Milner[1,3], Adam E Jakus[4,5], Ramille N Shah[4], Sierra A Long[1], Paula V Marchioretto[1], Jonathon Burke[4], Matthew B Wheeler[1,2,3,5*]

[1]Department of Animal Sciences, University of Illinois at Urbana-Champaign, Urbana, IL 61801, USA
[2]Carl R. Woese Institute for Genomic Biology, University of Illinois at Urbana-Champaign, Urbana, IL 61801, USA
[3]Department of Bioengineering, University of Illinois at Urbana-Champaign, Urbana, IL 61801, USA
[4]Dimension Bio, Corp, Chicago, IL 60616; 5 BioThera3 Advising and Consulting, Chicago, IL, USA
[5]Department of Biomedical and Translational Sciences Carle-Illinois College of Medicine, USA
***Correspondence author:** Matthew B Wheeler, Ph.D., University of Illinois, 1207 West Gregory Drive Urbana, IL 61801; Email: mbwheele@illinois.edu

Citation: Milner JD, et al. CMFlex® Bone Graft Accelerates Bone Formation and Contour Recovery in Multi-Centimeter Porcine Mandibular Defects: A Pilot Study. J Reg Med Biol Res. 2026;7(2):1-12.

https://doi.org/10.46889/JRMBR.2026.7205

Received Date: 07-07-2026

Accepted Date: 27-07-2026

Published Date: 03-08-2026

Abstract

Background: This study aimed to evaluate the performance of CMFlex® bone grafts in regenerating bone and restoring anatomical contour of large, irregular mandibular defects in a porcine model.

Methods: Two adult (6-9 months of age) Yorkshire pigs with ramus defects (~12.7 cm^2 area), treated with CMFlex® bone grafts (experimental) or left untreated (negative control). Animals were euthanized at 16- and 32-weeks post-implantation. Bone regeneration was assessed using CT, micro-CT, histology and mechanical testing to evaluate new bone formation, scaffold integration and contour restoration.

Findings: CT imaging showed that CMFlex® grafts promoted significant bone formation, with substantial defect filling by 12-16 weeks. Two out of three defects successfully restored the jawline contour, while the third showed partial extrusion of new bone due to scaffold displacement. Micro-CT imaging confirmed scaffold material integrated within the bone and surrounding tissues at both time points. Histological analysis revealed active bone formation and maturation around and within the scaffold, along with evidence of scaffold degradation. Mechanical testing via nanoindentation showed no significant difference in Young's Modulus between regenerated bone and native bone, suggesting comparable mechanical properties.

Conclusion: This pilot study demonstrates that CMFlex® bone grafts can effectively regenerate bone in large (>5 cm^2, which is ~25 mm diameter) mandibular defects and restore anatomical contour. These findings support the potential of CMFlex® as a promising scaffold-based solution for large-scale bone defects in human patients, warranting further clinical investigation.

Keywords: Bone Graft; Mandibular Defect; Porcine Model; Bone Contour; Scaffold

Abbreviations

3D: Three-Dimensional; AAALAC: American Association for Accreditation of Laboratory Animal Care; ANOVA: Analysis of Variance; CMFlex®: Novel Regenerative Bone Graft; CO_2: Carbon Dioxide; CT: Computed Tomography; FDA: Food and Drug Administration; GenAI: Generative Artificial Intelligence; GPa: Gigapascal; ISRL: Imported Swine Research Laboratory; IACUC: Institutional Animal Care and Use Committee; kEV: kiloelectronvolt; kg: kilograms; MMA: Methylmethacryate; µCT: micro-Computed Tomography; Micro-CT: micro-Computed Tomography; mA: milli-Amp; PRL: Physiology Research Laboratory; PLG: Polylactide-Co-Glycolide: TARK: Telazol-Atropine-Rompun-Ketamine anesthetic cocktail

Introduction

Facial and jaw injuries-whether resulting from congenital anomalies, trauma or disease-often lead to profound functional and aesthetic impairments, presenting significant challenges for effective reconstruction. The complex anatomy of facial bones complicates efforts to restore both form and function, with current methods often falling short. Repairing large and/or complex bone and bone-cartilage defects remains one of the most formidable challenges in both craniofacial and orthopedic surgery. These defects are highly patient-specific, requiring tailored, precise solutions to optimize outcomes.

Traditionally, the most common grafts for these repairs-autografts and allografts-demand significant surgical skill and time. Autografts require harvesting tissue from the patient's own body, which can cause pain or complications at the donor site, while allografts and xenografts introduce risks of disease transmission, immunological reactions and inconsistency in material properties. These limitations underscore the urgent need for more reliable, efficient and customizable synthetic alternatives.

CMFlex® is a novel regenerative bone graft that offers a solution to these long-standing challenges. It is the first FDA-cleared 3D-printed regenerative bone graft specifically indicated for oral and maxillofacial use and the first commercial product made from Hyperelastic Bone® [1-3]. Comprising 90% calcium phosphate and 10% biodegradable Polylactide-Co-Glycolide (PLG), CMFlex® is a fully synthetic solution that harnesses its unique microstructure to control cell behavior, promote bone regeneration and facilitate cell, tissue and blood vessel infiltration, which are essential for implant stabilization and long-term viability.

Unlike autografts and allografts, CMFlex® eliminates the need for painful harvesting and the risks associated with tissue variability and disease transmission. Although CMFlex® is comprised of majority ceramic, its unique flexibility offers surgeons an easy-to-shape material that can be tailored to fit the defect site (i.e., with a surgical scalpel), reducing preparation time in the operating room. Additionally, because CMFlex® is produced using 3D printing, it is possible to create patient-specific regenerative bone grafts based on individual scans. This capability is gaining interest in the oral and maxillofacial field, though CMFlex® is not yet for patient-specific implants. The aim of this study was to assess the bone healing (via computed tomography and histology), mechanical properties of the healed bone (via nanoindentation) and mandibular contour recovery (via computed tomography and visual observation) of CMFlex® in a large volume full thickness bone defect using a porcine model, providing crucial insights into its potential as a revolutionary solution for reconstructive surgery.

Materials and Methods

Material and 3D-Printed Scaffold Preparation

CMFlex® is manufactured using a 3D-printing process involving Hyperelastic Bone® ink that is composed of two functional components - hydroxyapatite powder (90% w/w solids, average particle size of 25 μm, Merz Biomaterials) and polylactide-co-glycolide (PLG (85:15 PL to PG ratio), 10% w/w solids (out of the total weight of the mixture, 10% of it is made up of solid material and 90% is liquid or solvent), Evonik) - alongside three solvents (comprising Dichloromethane (DCM; evaporant), 2-Butoxyethanol (2-Bu; surfactant) and Dibutyl Phthalate (DBP; plasticizer) that facilitate subsequent processing as previously described [1-3]. Briefly, the manufacturing process begins with the dissolution of the polymer in one of the solvents (DCM) until the solution is homogenous. The ceramic and the remaining solvents are then introduced into this solution, followed by further homogenization. The resulting mixture, now the "ink", is then distributed into cartridges intended for extrusion-based 3D printing. Utilizing a 22-gauge nozzle, the material is printed at room temperature using an EnvisionTEC 3D BioPlotter following a pattern of successive, advancing 120 Deg angles characterizing each layer (i.e. 0-120-240-0-120-240 with a 1.4 mm spacing between strands. The device is printed layer-by-layer with each layer drying quick enough to ensure adhesion of the subsequent layer. The final shape and dimensions of the implant, which was chosen to demonstrate the ability to create a more patient-specific complex device, are presented in Fig. 1A. This form was further selected as it is characterized by both convex and concave surfaces and can also fit a defect that can be reliably and consistently produced using standard trephines (i.e. one large circular void with an additional two smaller voids overlapping with the larger). We have previously established that a > 25 mm defect in the ramus of the pig mandible is a critical size defect [4]. Upon completion of the printing process, the device undergoes a series of washing steps in alcohol and water to eliminate excess solvents, followed by a lyophilization step to remove residual moisture. Finally, the device is initially packaged in a breathable pouch and sterilized using supercritical CO_2 with peracetic acid-based sterilant. After an outgassing period, the device packaging undergoes final sealing prior to shipment and use.

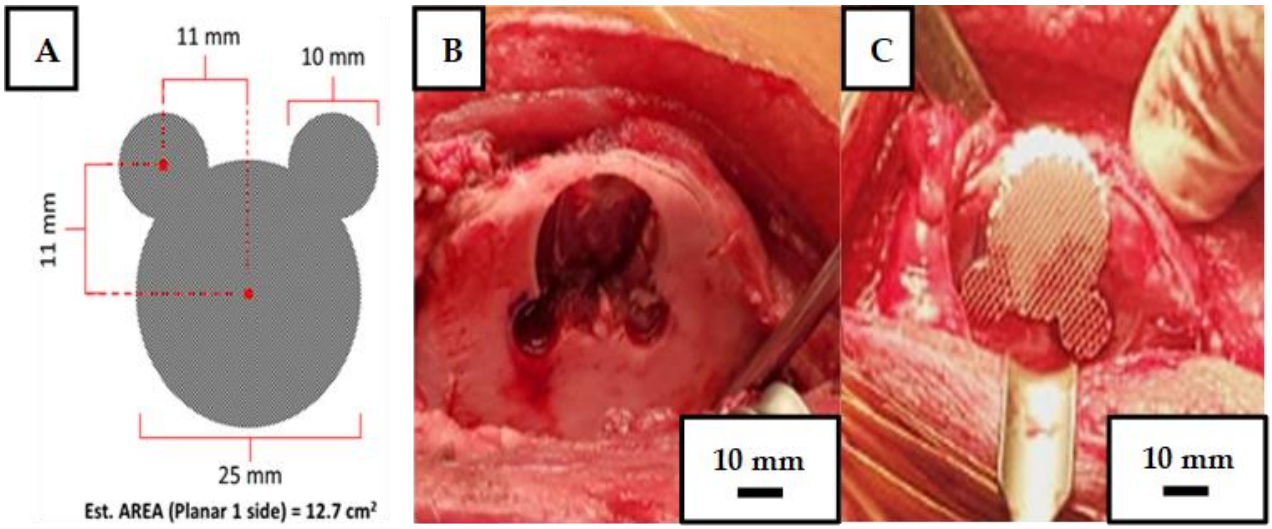

Figure 1: (A) Schematic of CMFlex® implant dimensions (for clarity the diagram is shown ~3 times the actual size of the implants in Panels B and C; (B) Photo of defect site in the ramus for empty control. Note a bone bridge was left on greater curvature of the ramus to provide greater stability; (C) Photo of defect site including excision of the greater curvature of the ramus after CMFlex® graft implantation. Note blood wicking into the CMFlex® porosity immediately after implantation.

Surgical Procedure

Experiments involving the use of animals were conducted in accordance with protocols approved by the University of Illinois Animal Care and Use Committee (IACUC Protocol #21019). Castrated male Yorkshire pigs (barrows), a well understood model with known clinical relevance were purchased from the Imported Swine Research Laboratory (ISRL) at the University of Illinois at Urbana-Champaign and maintained in the biomedical section of ISRL for up to 18 months (pre- and post-implant surgery time). Mature pigs (~6-9 months of age, 100-200 kg) were used for the study [4-14].

Before surgery, all pigs received a sedative cocktail (TARK) consisting of Telazol (tiletamine and zolazepam; Pfizer, New York, NY), Atropine (Neogen Corporation, Lexngton, KY), Rompun (xylazine; Lloyd Laboratories, Shenandoah, IA) and Ketamine (Ketaset®; Fort Dodge Animal Health, Fort Dodge, IA) intramuscularly, then again intravenously via the ear vein canula, as necessary. Additionally, endotracheal administration of 3-5% isoflurane was administered in oxygen as anesthesia during surgery [4]. To prep for the surgical procedure, the animal was first draped to provide the sterile operating field. Using aseptic surgical technique an incision was made on the exterior contour of the mandible with a scalpel blade. The skin, superficial fat and muscle were incised and the periosteum of the mandible exposed [5,13]. Dissection through soft tissue planes was carried out exposing the entire inferior border of the mandible from the parasymphyseal region, posterior, to the angle of the mandible. A subperiosteal flap was developed on the lateral aspect of the body of the mandible. The periosteum was elevated and the pre-determined, full thickness, mandibular bone defect, in the load-bearing area of the mandible (ramus and posterior alveolar segment), was created with a power drill using a trephine under copious irrigation (Fig. 1B). One defect (~12.7cm2 area) in each hemi-mandible was created near and including the greater curvature of the ramus for sites where CMFlex® was implanted (Fig. 1C). For the empty defect control site, a piece of bridging bone at the greater curvature of the ramus was left to allow for greater mechanical stability (Fig. 1B). Defects were 10-12 mm in depth located within the ramus portion of the mandible bone. CMFlex® implants were inserted into each hemi-mandible, as appropriate and the periosteum, muscle, superficial fat and skin were closed over the defects and implants in a layered fashion with 2-0 or 3-0 absorbable sutures.

Animals were returned to a clean, dry pen to recover and were maintained on a soft diet for 2 to 7 days or longer as appropriate. Animals were recovered for a 1-7-day period in the Physiology Research Lab (PRL) at the University of Illinois at Urbana-Champaign and then returned to the ISRL and tended with humane care consistent with standard practices of that AAALAC Accredited facility. One pig containing CMFlex® on one side of the mandible and an empty defect on the other side of the mandible was sacrificed at 16 weeks post implant. The second pig containing CMFlex® on both sides of the mandible was sacrificed at 32 weeks.

Computed Tomography (CT) and Micro-Computed Tomography (micro-CT) Imaging

CT scans were taken of live pigs at 4-week intervals *in-vivo* after implantation of CMFlex® bone grafts [15]. Prior to imaging, animals were first sedated with a sedative cocktail (TARK) as described in surgical procedures. Pig skulls were scanned using a Lightspeed 16 slice Helical CT scanner (General Electric, Fairfield, CT) at 140 kEV and 240 mA.

Post sacrifice and prior to processing for histology, jaw segments containing the implant area were scanned using micro-CT via a NSI X5000 3D CT system (North Star Imaging, Rogers, MN). Jaw samples were scanned at 65kV of voltage, 80 μA of current under step motion in a microfocus mode and framerate of 7.5 fps. Reconstructed three-dimensional volume had a size of 1232 x 1829 x 1232 voxels, providing an isotropic spatial resolution of 53.5 microns voxel-1 and a 16-bit intensity range. This enabled the identification of both bone matrix tissue and more opaque regions of implants. The number of projections collected for each individual jaw was 2520 and were used to build a three-dimensional volume model by reconstruction using efX-ct software (version 2.2.5, North Star Imaging Inc., Rogers, MN).

Histology

Mandibles were dissected out of euthanized pigs and the region of the mandible containing the implant was isolated using a band saw [15]. The implant segments were fixed in 10% neutral buffered formalin, rinsed with phosphate buffered saline, then embedded in Methyl Methacrylate (MMA) using standard procedures [5]. After additional trimming, MMA embedded samples were sectioned using a diamond blade on a Buehler Isomet 1000 precision saw (Buehler, Lake Bluff, IL). Sections were cut at a thickness of 0.5 -1.0 mm and glued to plastic backing using cyanoacrylate adhesive. After adhesion overnight, sections were ground and polished with a series of silicon carbide sanding paper ranging from 100 grit to 1200 grit on a Buehler Ecomet grinder/polisher (Buehler, Lake Bluff, IL) with water irrigation to remove debris and prevent burning/melting. After polishing, sections were stained with Sanderson's Rapid Bone Stain, then imaged using a Zeiss AxioZoom V16 Microscope (Zeiss, White Plains, NY) [5].

Mechanical Property Measurements of Explants

A Hysitron TI950 TriboIndenter was used to perform nanoindentation measurements and obtain Young's Modulus of native bone and regenerated bone in the implant regions. Ten indentations were made on regions of unaltered and new bone in 3 separate sections of each bone type. Histological sections were adhered to steel plates using cyanoacrylate adhesive to affix samples to the magnetized stage of the nanoindenter. A standard load transducer using a diamond Berkovich tip was used to deliver a 1000 μN controlled load indent using a QS trapezoid load function. Young's Modulus values were calculated from the resulting load displacement curves for each indent.

Statistical Analysis

Elastic modulus of the native (unaltered control) bone and the newly formed (healed bone) were analyzed by ANOVA (SAS, 2025) for the main effect of bone strength measured via nanoindentation. The alpha value was set at 0.05.

Results

Monitoring of Bone Healing in vivo by CT Imaging and Examination of Jaw Segments

Healing of the jaw defects was monitored *in-vivo* by whole-head CT imaging scans performed at 4-week intervals. The 16-week pig received a CMFlex® graft in the left side defect, while the right-side defect was left empty. On the left side, bone ingrowth is clearly observable in the defect by 4 weeks. By 12 weeks, bone growth has filled most of the defect and the contour of the jaw has been roughly re-established (Fig. 2). In contrast the right side, which did not receive a graft, showed little healing even by 8 weeks. By 12 weeks, some healing of the defect had occurred, but the contour of the jaw had not been reformed. Instead, bony protrusions have formed around the center of the defect (Fig. 2).

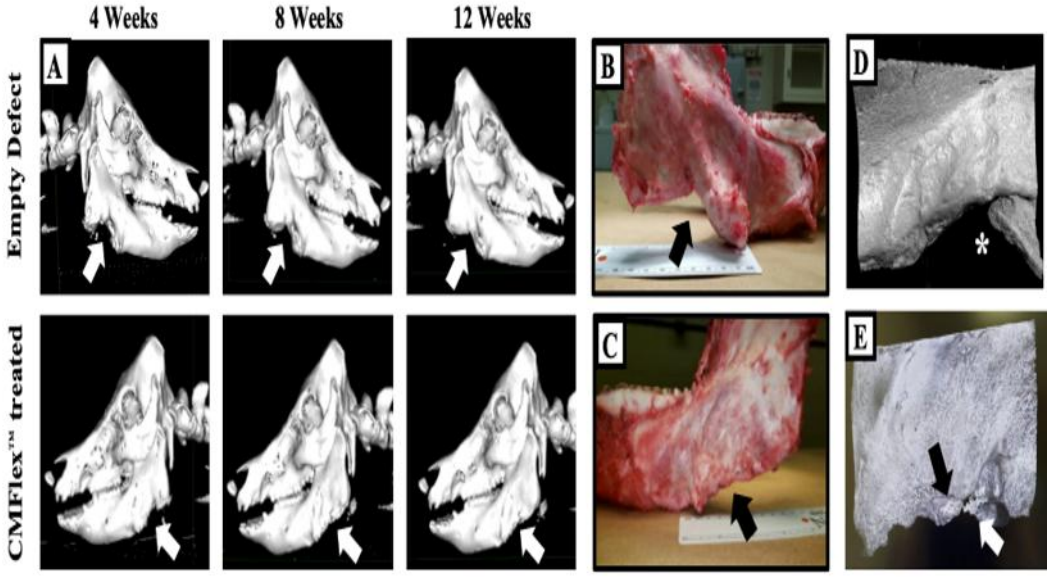

Figure 2: CT imaging and gross morphology of excised jaws of pigs at 16 weeks. (A) CT scans over time at 4, 8 and 12 weeks of the empty defect control (top row) and the CMFlex® treated defect (bottom row). (B) Right side of excised jaw, without an implant (negative control) and (C) left side of excised jaw with CMFlex® implant. Note the excised area in empty defect control (arrow) has not closed and the contour of the jaw has not been reestablished, which is also observed in CT scans. In contrast, the defect in the right side of the jaw that received the CMFlex® implant (C) has been filled with new bone and the contour of the jaw has been essentially reestablished by between 8-12 weeks post-implantation as observed by CT imaging. (D) uCT imaging of the empty defect explant and (E) CMFlex® treated explant post-harvest. Note confirmation of the gap in the empty defect control (asterisk), while the CMFlex® treated defect has been filled with new bone. Portions of residual scaffold are visible (arrows) with some of the scaffold material embedded in soft tissue lining the bone (white arrow) and some residual material integrated and sticking out of the regenerated bone (black arrow).

Gross examination of the mandible removed at 16 weeks confirmed the observations of CT imaging (Fig. 2). On the left side of the mandible, the defect that received the CMFlex® graft had filled in with bone and had generated a contour like the unaltered mandible (Fig. 2). Some small flakes of CMFlex® scaffold material could be observed slightly sticking out from some soft tissue that lined the underside of the regenerated defect. This was confirmed by micro-CT imaging (Fig. 2), as small pieces of graft material can be observed embedded in the bone (black arrow), while graft material is clearly seen external to the bone (white arrow). As observed by CT imaging, healing of the empty defect (right) side of the mandible did not fill the defect or restore the contour of the mandible (Fig. 2). The lack of bone growth in the empty defect was also confirmed by micro-CT (μCT) (Fig. 2). In this case, instead of contour restoration, bony structures formed that splayed out medially and externally from the jaw line (Fig. 2).

The 32-week sacrificed pig received CMFlex® grafts in defects on both the right and left side of the mandible. As with the 16-week pig, both defects were filled and the contour of the jaw was essentially re-established. Additional CT imaging performed at 32 weeks showed a similar degree of contour restoration compared to that at 16 weeks (Supplemental Digital Content Fig. S1). Upon gross examination of the explanted tissue, the left side defect was filled with bone and generated a contour resembling that of the native mandible, with a few small growths of soft tissue and bone on the surface (Supplemental Digital Content Fig. S1). On the right side of the mandible the defect was filled, but the contour was imperfect, as a "wing" of bone tissue was seen to protrude externally at the defect site (Supplemental Digital Content Fig. S1). Micro-CT imaging (Supplemental Digital Content Fig. S1) revealed that this structure contained a significant amount of scaffold material, with some embedded in the bone (Supplemental Digital Content Fig. 1) and some exposed in soft tissue underlying the jaw (Supplemental Digital Content Fig. 1F, black arrow). This protrusion is likely from the graft becoming partially dislodged at some point after implantation, but the graft was still able to direct healing of the defect.

Histology

Segments of the mandible that contained the CMFlex® implants were taken after μCT imaging and embedded in methyl methacrylate. Sections roughly 0.5 mm to 1.0 mm thick were cut on a diamond saw and stained using Sanderson's Rapid Bone Stain. Sanderson's stains soft tissue, osteoid and nuclei blue, while staining mature bone red. Histological examination of the implant region from the 16-week mandible (Fig. 3) confirms what was observed in μCT imaging. A significant amount of mature bone (red stained) was found in most of the defect space (Fig. 3). There were areas of intact scaffold material mostly found on the periphery of the jaw line in bone and soft tissue (Fig. 3). Histologically, intact scaffold struts in cross section display an easily recognizable morphology: Structures that are clusters of pale circular vesicle-like structures (hydroxyapatite particles) interspersed in a red-pinkish stained matrix (polymer). Of note is that residual scaffold structures that were less degraded seemed to be surrounded more by soft tissue (Fig. 3) and other structures that were more degraded (Fig. 3) were surrounded by more mature bone. Overall, there was a significant amount of regenerated bone formed in and around the scaffolding of the CMFlex® graft over the 16-week healing period.

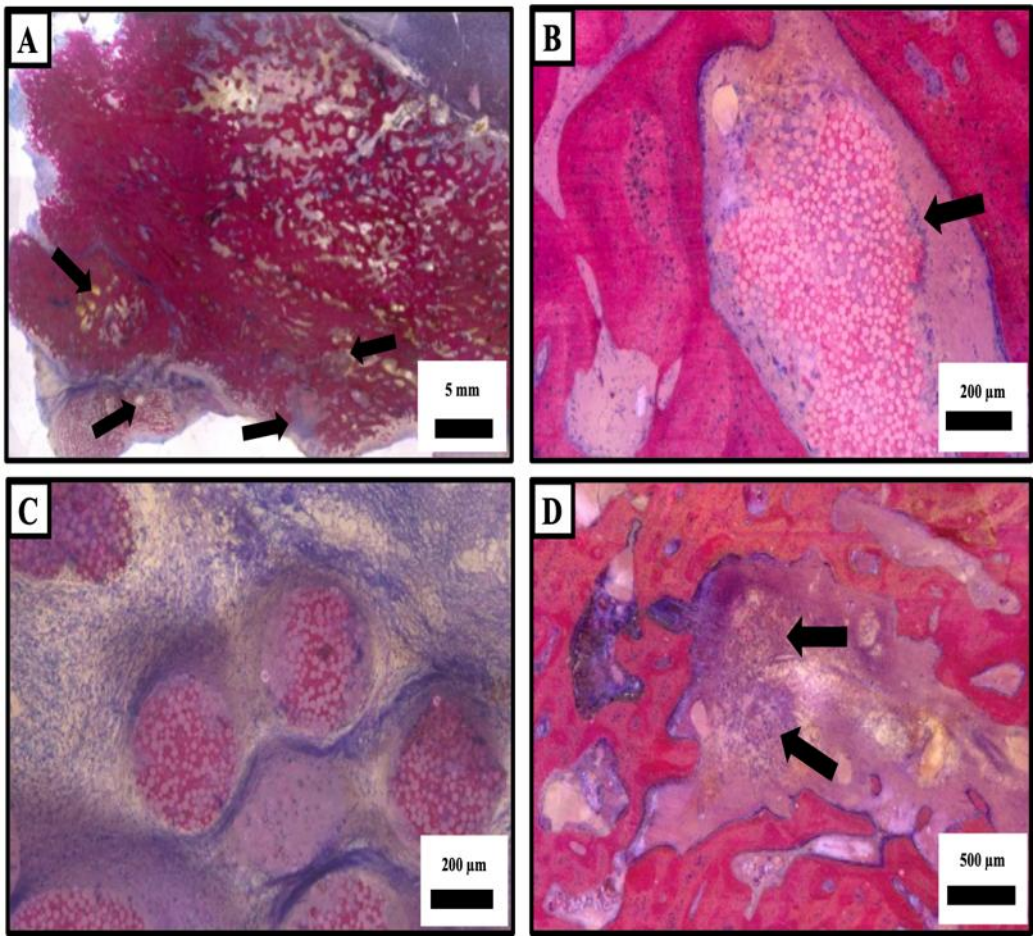

Figure 3: Histology of defect-implant area at 16 weeks post-surgical implantation of CMFlex® stained with Sanderson's Rapid Bone Stain. (A) Section of bone from implant region showing majority of defect treated with CMFlex® remodeled into mature bone (red staining). Arrows indicate where some residual scaffold material is left embedded within regenerated mature bone (arrows). (B) High magnification image of relatively intact scaffold material (arrow) surrounded by regenerated bone tissue. (C) Region where residual scaffold material was less degraded (near contour of jaw) showing different stages of fiber degradation and remodeling. In this region more collagen (blue) and immature regenerating bone is present. (D) Region where more advanced degradation of scaffold has occurred (arrows), showing presence of surrounding regenerating and more maturing bone.

Examination of sections of the mandible from 32 weeks show similar observations (Supplemental Digital Content Fig. S2). Histological analysis of the "wing" of bone tissue formed in the right mandible showed a significant amount of scaffold material embedded in this regenerated bone (Supplemental Digital Content Fig. S2), which was also observed in μCT imaging. An

unstained section of this structure shows multiple areas of scaffold material embedded in the bony structure (Supplemental Digital Content Fig. S2, arrows), including an area where the original geometric organization of the CMFlex® graft can still be observed (Supplemental Digital Content Fig. S2, white arrow). An adjacent section stained with Sanderson's (Supplemental Digital Content Fig. S2) shows scaffold segments surrounded by bone (Supplemental Digital Content Fig. 2, black arrows) and some scaffold material embedded in soft tissue lining the surface of the bone (Supplemental Digital Content Fig. S2, white arrow). The region highlighted by the black dashed box in Supplemental Digital Content Fig. S2 is shown in Supplemental Digital Content Fig. S2, clearly displaying CMFlex® graft material is completely integrated and surrounded by regenerated bone tissue.

Mechanical Property Measurements

A significant requirement for implants designed to promote bone growth and restore lost bone tissue is that they produce regenerated bone with mechanical properties like the native bone that they replace. To investigate the mechanical properties of bone produced by CMFlex® grafts, we performed nanoindentation testing on sections of bone isolated from implanted segments. We tested regions of bone on the margins of the excised mandible segments that had not been impacted by surgical manipulation and regions of bone formed surrounding and infiltrating CMFlex® graft material. Nanoindentation testing results are displayed in Fig. 4. Unaltered bone and regenerated bone were found to have similar values for Young's modulus in both the 16-week pig and the 32-week pig. These values are significantly higher than the modulus derived from measurements of areas of section containing no tissue and only MMA embedding media (5.07 GPa), indicating that we are measuring properties of the bone tissue and not the plastic matrix of the sections. While it is impossible to reliably determine macro-level mechanical properties from tissue sections, these micro-scale measurements suggest that the bone tissue regenerated in CMFlex® grafts have mechanical characteristics like the native bone it has replaced.

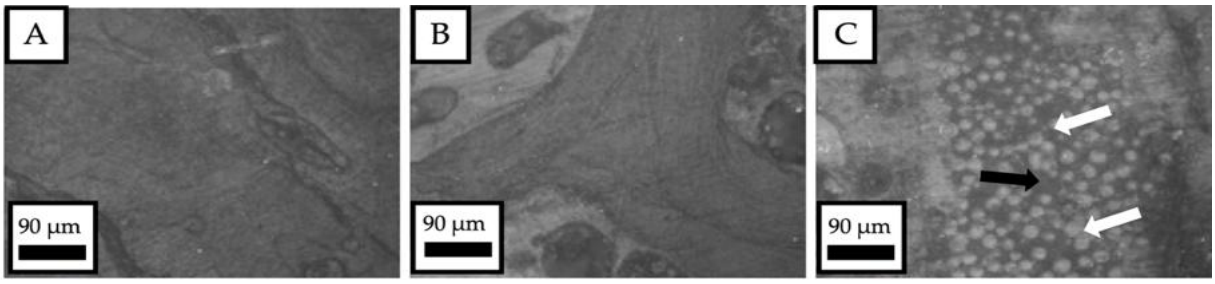

Elastic Modulus (E; GPa)					
Timepoint	**Unaltered Bone**	**New Bone**	**Scaffold (Vesicles)**	**Scaffold (Amorphous)**	**MMA**
16-Weeks	**10.631 ± 2.425**	**10.407 ± 1.061**	**66.294 ± 34.556**	**3.495 ± 1.663**	**5.704 ± 0.498**
32-Weeks	**12.301 ± 1.723**	**12.747 ± 1.976**	**65.094 ± 13.471**	**4.194 ± 1.187**	**5.115 ± 0.484**

Figure 4: Mechanical properties of regenerated bone as determined by nanoindentation. The elastic modulus was measured in Gigapascals (GPa). Regions of undisturbed bone (A) and regenerated bone (B) were probed by nanoindentation utilizing a Berkovich diamond tip. (C) Region where intact fiber is apparent with hydroxyapatite particles (white arrows) embedded within residual polymer matrix (black arrow) was also analyzed. Calculation of Young's Modulus (E) from nanoindentation data suggests that newly formed bone has similar mechanical properties as unaltered bone. Ten (10) indentations were made on regions of unaltered and new bone in 3 separate sections from the animal harvested after 32 weeks. Analysis by ANOVA indicates that there is no statistically significant difference ($p>0.05$) between the moduli measured in new and unaltered bone ($p= 0.273$). Measurements were also taken in regions where embedding material, methyl methacrylate (MMA) resin, did not contain tissue.

Discussion

This pilot study evaluated the potential of a novel 3D-printed bone graft, CMFlex®, to regenerate bone and restore the jawline in large multi-centimeter defects in a porcine ramus model. Our findings demonstrate that CMFlex® is not only capable of being easily press-fit into large defects, but also effectively integrates with the surrounding bone, promoting substantial bone regeneration. Notably, the graft facilitated nearly complete recovery of the ramus contour within just 8 weeks post-implantation.

After 32 weeks, although some residual CMFlex® material remained in localized regions of the defect, the scaffold was completely integrated with the host bone and mature bone had bridged the entire defect, as confirmed by μCT imaging and histological analysis. These results highlight CMFlex® 's potential as a robust, self-sustaining scaffold that supports new bone formation without the need for exogenous stem cells, growth factors or other osteoinductive agents. Similar findings were seen in several other animal models (mouse, rat and non-human primate) were no exogenous cells, growth factors or osteogenic chemicals were used [1,2]. Importantly, the newly formed bone exhibited similar morphological and mechanical properties to the native surrounding bone, indicating successful bone maturation within the grafted area.

The observed efficacy of CMFlex® in regenerating bone in a multi-centimeter defect can be attributed to its unique structural characteristics. The material's open and interconnected microporosity (i.e., porosity within each printed fiber) promotes rapid cellular infiltration, providing an ideal environment for osteogenic activity. Moreover, the intrafiber porosity of the printed scaffold enhances the material's absorption properties, facilitating faster blood and protein absorption and improving cellular attachment-key factors in accelerating bone regeneration. The presence of accessible hydroxyapatite particles within the biodegradable polymer matrix creates a calcium- and phosphate-rich microenvironment as the scaffold degrades, further promoting mesenchymal stem cell differentiation into osteoblasts and supporting bone mineralization [3]. These mechanisms are consistent with the histological findings, which show that regions of the defect where CMFlex® had degraded were populated by mature bone, whereas areas with minimal degradation were still populated by collagenous connective tissue that had yet to mineralize (Fig. 3). Notably, the regions with more residual material tended to be located at the periphery of the implant at the edge of the jaw contour, likely due to this area being farther from the surrounding native bone-and consequently, further from the stem cell reservoir, which may have led to slower bone remodeling in this region.

Our results are especially significant when considered in the context of existing literature. Most studies on synthetic bone grafts in large, multi-centimeter defects, particularly in large animal models [16], typically require the addition of exogenous cells (e.g., mesenchymal stem cells), autologous bone or growth factors to achieve substantial bone formation across the entire defect volume [5,13,17-24]. In contrast, CMFlex® successfully facilitated significant bone regeneration without the need for additional biological stimuli, highlighting its ability to support bone healing on its own. This is a noteworthy advantage, as it simplifies the surgical process and reduces reliance on costly or time-consuming biologic adjuncts. Furthermore, CMFlex® outperforms many synthetic bone grafts regarding handling, particularly those composed predominantly of calcium phosphate materials, which tend to be brittle and difficult to shape. Unlike these materials, CMFlex® is compliant and can be easily shaped with a surgical scalpel without crumbling, allowing for better adaptation to complex defect sites [1]. These superior handling properties, in conjunction with its osteogenic capacity, position CMFlex® as a highly promising bone graft material for clinical applications.

Conclusion

Although this pilot study provides compelling evidence of CMFlex® 's effectiveness in regenerating bone in large mandibular defects in a porcine model, further research is warranted to confirm these findings in human clinical settings. Future studies should evaluate the long-term remodeling and bone-forming properties of CMFlex® in human patients and determine its biocompatibility and functional integration in human bone. Additionally, exploration of CMFlex® in different bone sites and defects of varying complexity will help establish its versatility and potential for broader clinical use. Based on the results of this pilot study, we are optimistic about CMFlex® 's potential as a next-generation synthetic bone graft material, capable of revolutionizing bone regeneration in challenging defects, including those in the mandible and beyond.

Conflict of Interest

Patents pertaining to this work have been filed: (i) Ceramic-containing bioactive inks and printing methods for tissue engineering (inventors: AEJ and RNS), issued 2023, (ii) Ink compositions for three-dimensional printing and methods of forming objects using the ink compositions (inventors: AEJ and RNS), issued March 2020. The other authors declare that they have no competing interests. AEJ and RNS are co-founders of and shareholders in Dimension Bio Corp., which develops and manufactures new advanced manufacturing compatible materials and devices for medical and non-medical applications. RNS currently serves as the Chief Science Officer of Dimension Bio Corp. AEJ currently serves as Founder and Principal of BioThera3 Advising & Consulting as well as CEO of PRO Therapeutics. AEJ and RNS are inventors on patents that are licensed to Dimension Bio Corp. DJM, SAL, PVM AND MBW have no conflicts of interest.

Funding Statement
This work was partially supported by: USDA Multistate Research Project W-1371, W-5171 (ILLU-538-393) and partially by Dimension Bio, Corp, Chicago, IL 60616.

Acknowledgement
The authors thank the staff, especially Mr. Jonathan Mosely, the Unit Manager, at the Imported Swine Research Laboratory for their diligent and uncompromising care of the animals.

Data Availability Statement
The entirety of the data described is included in the published article and supplemental materials.

Ethical Statement
Experiments involving the use of animals were conducted in accordance with protocols approved by the University of Illinois Animal Care and Use Committee (IACUC Protocol #21019). Pigs were humanely euthanized at the Department of Animal Sciences' Physiology Research Laboratory. The procedures followed in this study were in accordance with the standards set forth in the eighth edition of "Guide for the Care and Use of Laboratory Animals" grants.nih.gov/grants/olaw/guide-for-the-care-and-use-of-laboratory-animals_prepub.pdf published by the National Academy of Sciences, The National Academies Press, Washington, D.C.).

Informed Consent Statement
Not applicable.

Authors' Contributions
Conceptualization (A.E.J., R.N.S, M.B.W.); project administration (M.B.W.); investigation (M.B.W, D.J.M., P.V.M., S.A.L.), methodology (A.E.J., R.N.S, D.J.M., M.B.W); data curation (M.B.W., D.J.M.); data analysis (M.B.W., D.J.M, A.E.J.), literature search (M.B.W., D.J.M.); (writing-original draft preparation (M.B.W., D.J.M.), writing-review and editing (A.E.J., R.N.S, D.J.M., J.B., M.B.W.); supervision (M.B.W.); resources and funding acquisition (M.B.W., R.N.S.). All authors have read and agreed to the published version of the manuscript.

References
1. Huang YH, Jakus AE, Jordan SW, Dumanian Z, Parker K, Zhao L, et al. Three-dimensionally printed hyperelastic bone scaffolds accelerate bone regeneration in critical-size calvarial bone defects. Plast Reconstr Surg. 2019;143:1397-407.
2. Jakus AE, Rutz AL, Jordan SW, Kannan A, Mitchell SM, Yun C, et al. Hyperelastic bone: A highly versatile, growth factor-free, osteoregenerative, scalable and surgically friendly biomaterial. Sci Transl Med. 2016;8:358ra127.
3. Dewey MJ, Nosatov AV, Subedi K, Shah R, Jakus A, Harley BAC. Inclusion of a 3D-printed hyperelastic bone mesh improves mechanical and osteogenic performance of a mineralized collagen scaffold. Acta Biomater. 2021;121:224-36.
4. Dewey MJ, Milner DJ, Weisgerber D, Flanagan CL, Rubessa M, Lotti S, et al. Repair of critical-size porcine craniofacial bone defects using a collagen-polycaprolactone composite biomaterial. Biofabrication. 2022;14:014102.
5. Maki AJ, Rabel RAC, Rubessa M, Ercolin AC, Roballo KS, Cooper JJ, et al. Autologous adipose-derived stem cells, platelet-rich plasma and fibrin enhance healing of mandibular bone defects in swine. Int J Regen Med. 2020;3:2-9.
6. Maki AJ, Rabel RAC, Wheeler MB. Calcium phosphate treatment enhances osteogenic differentiation of porcine adipose-derived stem cells on fibrin scaffolds. Int J Regen Med. 2023;6:2-10.
7. Maki AJ, Rabel RAC, Wheeler MB. In vitro migration of porcine adipose-derived stem cells in platelet-rich plasma. Int J Regen Med. 2023;6:2-9.
8. Milner DJ, Bionaz M, Monaco E, Cameron JA, Wheeler MB. Myogenic potential of mesenchymal stem cells isolated from porcine adipose tissue. Cell Tissue Res. 2018;372:507-22.
9. Monaco E, Bionaz M, Hollister SJ, Wheeler MB. Strategies for regeneration of bone using porcine adult adipose-derived mesenchymal stem cells. Theriogenology. 2011;75:1381-99.
10. Monaco E, Bionaz M, Maki AJ, Wilson SM, Hurley WL, Wheeler MB. Morphological and transcriptomic comparison of adipose- and bone marrow-derived porcine stem cells. Open Tissue Eng Regen Med J. 2009;2.

11. Phillips RW, Tumbleson ME. Models in swine biomedical research. In: Tumbleson ME, editor. Swine in Biomedical Research. Vol. 1. New York: Plenum Press. 1986:437-40.
12. Prather RS. Swine as a biomedical model. In: Advantages of Agriculturally Important Domestic Species as Biomedical Models. Proceedings of the NIH NCRR Workshop. 2004.
13. Wilson SM, Goldwasser MS, Clark SG, Monaco E, Bionaz M, Hurley WL, et al. Adipose-derived mesenchymal stem cells enhance healing of mandibular defects in the ramus of swine. J Oral Maxillofac Surg. 2012;70:e193-e203.
14. Wilson SM, Goldwasser MS, Clark SG, Monaco E, Rodriguez-Zas S, Hurley WL, et al. Adipose-derived stem cell migration in the vascular system after transplantation and the potential colonization of ectopic sites in swine. J Regen Med Biol Res. 2021;2:1-6.
15. Weisgerber DW, Milner DJ, Lopez-Lake H, Rubessa M, Lotti S, Polkoff K, et al. A mineralized collagen-polycaprolactone composite promotes healing of a porcine mandibular defect. Tissue Eng Part A. 2018;24:943-54.
16. Hatt LP, Thompson K, Helms JA, Stoddart MJ, Armiento AR. Clinically relevant preclinical animal models for testing novel cranio-maxillofacial bone 3D-printed biomaterials. Clin Transl Med. 2022;12:e690.
17. Probst FA, Fliefel R, Burian E, Probst M, Eddicks M, Cornelsen M, et al. Bone regeneration of minipig mandibular defects using adipose-derived mesenchymal stem cells seeded on tricalcium phosphate-poly(D,L-lactide-co-glycolide) scaffolds. Sci Rep. 2020;10:2062.
18. Rubessa M, Polkoff K, Bionaz M, Monaco E, Milner DJ, Hollister SJ, et al. Use of pigs as a model for mesenchymal stem cell therapies for bone regeneration. Anim Biotechnol. 2017;28:275-87.
19. Rohner D, Hutmacher DW, Cheng TK, Oberholzer M, Hammer B. *In-vivo* efficacy of bone marrow-coated polycaprolactone scaffolds for reconstruction of orbital defects in pigs. J Biomed Mater Res B Appl Biomater. 2003;66:574-80.
20. Bhumiratana S, Bernhard JC, Alfi DM, Yeager K, Eton RE, Bova J, et al. Tissue-engineered autologous grafts for facial bone reconstruction. Sci Transl Med. 2016;8:343ra83.
21. Carstens MH, Chin M, Li XJ. In situ osteogenesis: Regeneration of a 10-cm mandibular defect in a porcine model using recombinant human bone morphogenetic protein-2 and Helistat absorbable collagen sponge. J Craniofac Surg. 2005;16:1033-42.
22. Springer ING, Acil Y, Kuchenbecker S, Bolte H, Warnke PH, Abboud M, et al. Bone graft versus BMP-7 in a critical-size defect: Cranioplasty in a growing infant model. Bone. 2005;37:563-9.
23. Wehrhan F, Amann K, Molenberg A, Lutz R, Neukam FW, Schlegel KA. PEG matrix enables cell-mediated local BMP-2 gene delivery and increases bone formation in a porcine critical-size craniofacial defect model. Clin Oral Implants Res. 2012;23:805-13.
24. Liu T, Fang W, Wu G, Li Y, Pathak JL, Liu Y. Low-dose BMP2-doped calcium phosphate graft promotes bone defect healing in a large animal model. Front Cell Dev Biol. 2021;8:613891.

Supplementary Materials

Fig. S1: CT imaging and gross morphology of excised jaws of pigs at 32 weeks.

Fig. S2: Histology of defect-implant area at 32 weeks post-surgical implantation of CMFlex®.

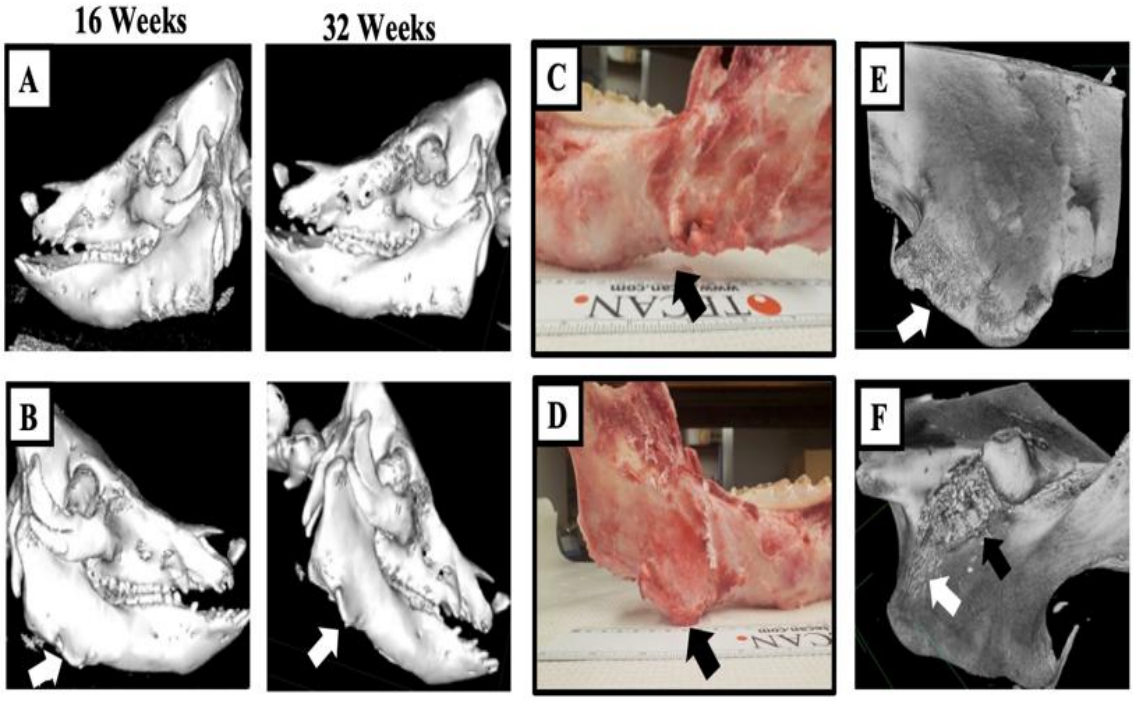

Figure S1: CT imaging and gross morphology of excised jaws of pigs at 32 weeks. (A) CT scans at 16 and 32 weeks of left (A) and right (B) side of the jaw both containing CMFlex® implants. The defect was filled with new bone on the left side and the contour of the jaw has essentially been reestablished at 16 weeks with little difference after 32 weeks. Gross morphology of the left side (C) after explantation confirms recovery of the contour. The defect in the right side of the jaw was also filled with new bone at 16 weeks, but a "wing" of bone tissue was also formed in the implant region extruding from the surface of the jaw (white arrow) with little difference after 32 weeks. Gross morphology of the right side (D) after explantation confirms this protrusion. uCT imaging of the formed "wing" on the right side (E) and (F) indicates residual CMFlex® material is embedded in this wing of bone tissue (white arrow), with a portion of the scaffold material sticking out of the bone (black arrow).

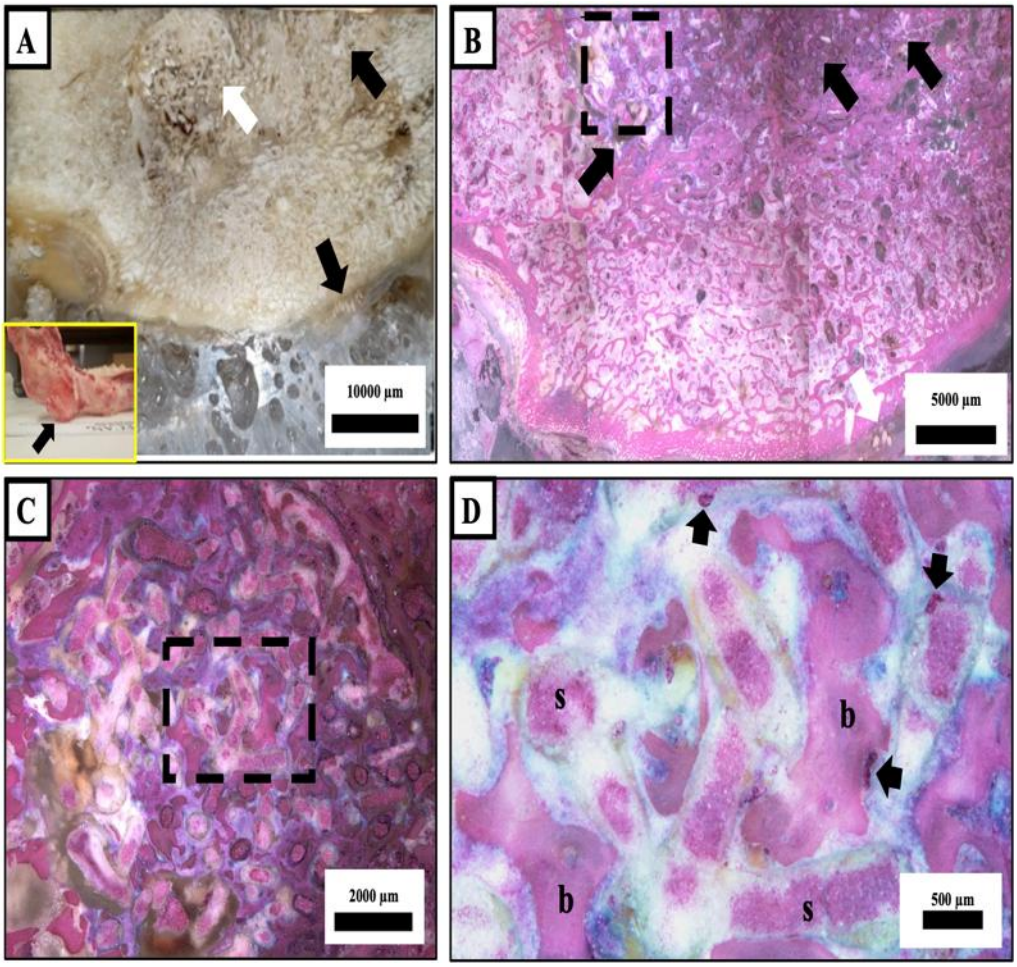

Figure S2: Histology of defect-implant area at 32 weeks post-surgical implantation of CMFlex®. (A) Unstained MMA section of bone taken from the wing of bone tissue formed at the implant site in the right mandible (A inset; Figure 3D) showing the presence of scaffold material embedded in the regenerated bone (arrows); (B) Sanderson's-stained section from (A) revealing bone tissue and remaining embedded scaffold material (arrows); (C) Enlarged image from the hatched box in (B) demonstrating presence of scaffold material surrounded by regenerated bone.